Published in final edited form as:
Transplantation. 2009 April 15; 87(7): 983–991. doi:10.1097/TP.0b013e31819c86ea.

Human β-cell Precursors Mature Into Functional Insulin-producing Cells in an Immunoisolation Device: Implications for Diabetes Cell Therapies

Seung-Hee Lee[1,2], **Ergeng Hao**[3], **Alexei Y. Savinov**[4], **Ifat Geron**[3], **Alex Y. Strongin**[4], and **Pamela Itkin-Ansari**[1,2,3,5]

[1]Development and Aging Program, Burnham Institute for Medical Research, La Jolla, CA

[2]Sanford Children's Health Research Center, Burnham Institute for Medical Research, La Jolla, CA

[3]Departments of Pediatrics and Moores Cancer Center, University of California, San Diego La Jolla, CA

[4]Infectious and Inflammatory Diseases Program, Burnham Institute for Medical Research, La Jolla, CA

Abstract

Background—Islet transplantation is limited by the need for chronic immunosuppression and the paucity of donor tissue. As new sources of human β-cells are developed (e.g., stem cell-derived tissue), transplanting them in a durable device could obviate the need for immunosuppression, while also protecting the patient from any risk of tumorigenicity. Here, we studied (1) the survival and function of encapsulated human β-cells and their progenitors and (2) the engraftment of encapsulated murine β-cells in allo- and autoimmune settings.

Methods—Human islets and human fetal pancreatic islet-like cell clusters were encapsulated in polytetrafluorethylene devices (TheraCyte) and transplanted into immunodeficient mice. Graft survival and function was measured by immunohistochemistry, circulating human C-peptide levels, and blood glucose levels. Bioluminescent imaging was used to monitor encapsulated neonatal murine islets.

Results—Encapsulated human islet-like cell clusters survived, replicated, and acquired a level of glucose responsive insulin secretion sufficient to ameliorate hyperglycemia in diabetic mice. Bioluminescent imaging of encapsulated murine neonatal islets revealed a dynamic process of cell death followed by regrowth, resulting in robust long-term allograft survival. Further, in the non-obese diabetic (NOD) mouse model of type I diabetes, encapsulated primary β-cells ameliorated diabetes without stimulating a detectable T-cell response.

Conclusions—We demonstrate for the first time that human β-cells function is compatible with encapsulation in a durable, immunoprotective device. Moreover, our study suggests that encapsulation of β-cells before terminal differentiation will be a successful approach for new cell-based therapies for diabetes, such as those derived from stem cells.

Keywords

Encapsulation; Diabetes; Islet transplantation; Immunoisolation

5Address correspondence to: Pamela Itkin-Ansari, Ph.D., Department of Pediatrics, University of California San Diego, 9500 Gilman Dr, MC 0816, La Jolla, CA 92093-0816, E-mail: E-mail: pitkinan@ucsd.edu.

The success of islet transplantation for the treatment of type I diabetes is hindered by the need for chronic immunosuppression. There is an evidence that immunosuppressive drugs not only increase patient morbidity from infectious diseases and malignancy, but also exert dysregulatory effects on the process of β-cell regeneration (1). Encapsulation of cellular transplants has the potential to reduce or eliminate the need for immunosuppression. The technology can be divided into two major categories: microencapsulation and macroencapsulation. Both types consist of semipermeable membranes that allow for the diffusion of nutrients and therapeutic molecules, such as insulin, while preventing the free exchange of cells (2–4). The majority of islet encapsulation studies to date have been performed with microcapsules which contain one or a few islets, thereby providing a beneficial surface or volume ratio for diffusion (5). Multiple issues, however, impact the choice of an encapsulation modality for β-cell replacement.

The paucity of available tissue for islet transplantation has stimulated efforts to derive human β-cells from alternate sources such as stem cells. Concern that stem cell-derived tissue may harbor undifferentiated cells with tumorigenic potential or that cells expanded ex vivo may acquire tumorigenicity has been raised as an objection to their clinical use (6). This issue was highlighted by evidence that embryonic stem cells cultured in vitro undergo selection for growth promoting genetic events such as c-myc amplification (7). Microencapsulation seems an unsuitable treatment option because the microcapsules are synthesized from semi-solid materials such as alginate and poly ethylene glycol (PEG) (8,9) with unavoidable capsule breakage over time (10). In contrast, a durable immunoprotective device could serve as a platform for safely administering ex vivo-derived cell therapies.

The TheraCyte macroencapsulation device is a planar pouch featuring a bilaminar polytetrafluorethylene membrane system. The outer layer promotes tissue integration, whereas an inner, cell impermeable, membrane has a 0.4 μm pore size (11). The durability of this encapsulation device has been exploited to sequester transformed cells in cancer vaccine studies (12,13). Moreover, its subcutaneous placement allows cells to be transplanted in a minimally invasive manner and retrieved if necessary (12). The device is biologically inert and when transplanted into human patients for a year, there were no adverse effects (14).

The immunoprotective qualities of the device in allograft and autoimmune settings have been examined in limited, qualitative studies in which the degree of tissue survival was not measured (14–16). When a transformed murine β-cell line was encapsulated and transplanted into the NOD mouse model of type I (autoimmune) diabetes, cells survived, but it is unclear whether immunoprotection was complete or whether the proliferative rate of the cell line simply outpaced destruction by the immune system. Therefore, it is important that the survival and function of encapsulated primary β-cells, which exhibit limited proliferative capacity, be quantitated in allo-and autoimmune environments. Early reports that the device provided xenograft protections (17–19) were not confirmed by others, including the device manufacturers (20–22, and Pamela Itkin-Ansari, personal communication).

Human β-cell encapsulation poses a particular challenge, because of the extreme sensitivity of islets to hypoxic environments, such as exist in the early posttransplant period, before new blood vessels form (23–25). Previously, we reported that a cell line derived from human islets is capable of long-term survival inside the TheraCyte device (26). Thus, we wanted to extend those studies to primary human β-cells. Interestingly, islet-like cell clusters (ICCs) from 18- to 24- week human fetal pancreas, rich in endocrine progenitors, frequently function better in transplantation models than mature human islets (27,28). This study was designed to test the hypothesis that macroencapsulated human β-cell precursors transplanted into severe combined immunodeficiency (SCID) mice can survive and mature into functional β-cells in vivo. In

addition, we sought to apply bioluminescent imaging (BLI) to the measurement of encapsulated murine islet survival in real time in both allo- and autoimmune settings. The goal of the study is to identify a platform for the safe administration of stem cell-derived therapies.

MATERIALS AND METHODS

Tissue Preparation

Primary human islets were obtained from the NIH Islet Cell Resources (ICR)-Administrative and Bioinformatics Coordinating Center. Cells were cultured in 5.5 mM glucose Roswell Park Memorial Institute (culture medium)/10% fetal bovine serum/1% penicillin/streptomycin before transplantation. Human fetal pancreases at 18 to 24 gestational weeks were obtained from Advanced Bioscience Resource, CA. Cold ischemic time was 12 to 24 hr. Tissue procurement was arranged in accordance with University of California, San Diego (UCSD) institutional review board regulations. Human fetal ICCs were prepared as described previously (29). Briefly, pancreas was minced, digested with collagenase P (5.5 mg/mL, Roche, Switzerland), and cultured on low-adhesion plates (Costar Corning, NY) in Roswell Park Memorial Institute (culture medium)/10% fetal bovine serum/1% penicillin/streptozotocin, forming three-dimensional cell clusters. Five of seven preparations of fetal pancreatic cells led to measurable C-peptide in device transplants. Additionally, one animal transplanted with a sixth ICC preparation died 10 weeks after transplant under anesthesia. Immunohistochemistry of this explanted device revealed a similar increase in β-cell fraction.

Transgenic Friend Virus B (FVB)/N mice expressing luciferase from the β-actin promoter (FVB/N-Tg β-Actin-luc, Xenogen, CA) (30) are referred to as FVB^{luc}. Pancreases from luciferase positive and negative littermates were combined in equal numbers. Unpurified murine neonatal islets from 1- to 2-day-old mice were prepared as described for human ICCs. β-cells accounted for 10% of the cell preparations (see Figure, Supplemental Digital Content 1, http://links.lww.com/A931).

Device Preparation and Transplantation

TheraCyte encapsulation devices (TheraCyte Inc., CA) are comprised of an inner semipermeable membrane (pore size 0.4 μm), laminated to an outer membrane and covered by a loose polyester mesh (31). The devices are 2 cm long with an inner lumen of 4.5 μL. Sterile devices were prepared by following manufacturer's instructions by ethanol wetting and phospate-buffered saline washes. The device was loaded with cells using a Hamilton Syringe (Hamilton, NV), sealed with medical adhesive (Dow corning, MI), and implanted in dorsal subcutaneous space by blunt dissection in mice anesthetized with isoflurane. Control animals were transplanted with an equal number of unencapsulated cell clusters in the sub-capsular space of the renal compartment (RC) or dorsal subcutaneous space.

Human cells from multiple islet preparations were transplanted into 8-week-old SCID-Beige mice (Charles River, MA). The cell number in the islet fraction was estimated by doubling the β-cell fraction, based on the assumption that islets are comprised of approximately 50% β-cells, although human islet composition is variable. It has previously been determined that devices accommodate approximately 60 islets per μL luminal space (15,32,33). Therefore, 3 μL of packed ICCs loaded into 4.5 μL devices = 180 clusters, and a 19% β-cell fraction (38% islet fraction) in explant = approximately 70 islet equivalents (IEQs). For adult human islet transplants, 4.5 μL cells (270 clusters), 80% pure, were loaded into devices = 270×0.8 = approximately 216 IEQs. Data were reproducible across multiple islet preparations.

Supplemental digital content is available for this article. Direct URL citations appear in the printed text, and links to the digital files are provided in the HTML text of this article on the journal's Web site (www.transplantjournal.com).

Murine islet cells were transplanted into 5- to 10-week-old wtFVB, ICR (Harlan, IN) or NOD (Jackson Labs, ME) strain recipients. Devices containing 3 μL (180 clusters) of impure neonatal murine islets were estimated to contain a 26% β-cell fraction (52% islets) = approximately 94 IEQs. All animal procedures were approved by the Institutional Animal Care and Use Committee of the University of California San Diego and the Burnham Institute for Medical Research.

Diabetes Induction by Destruction of Endogenous β-Cells

Destruction of murine but not human β-cells in SCID mice was achieved by intravenous administration of 90 mg/kg alloxan (Sigma, MO) (34). Autoimmune diabetes was accelerated in NOD mice by a single intraperitoneal (IP) injection of low-dose streptozotocin (40 mg/kg in 0.1 M citrate pH 4 buffer, Sigma) as described previously (35,36). Blood glucose levels sampled from tail veins were monitored with a glucometer (MediSense, MA). Glucose stimulation and intraperitoneal glucose tolerance test were performed after overnight fast; blood samples were procured before and 30 min or more after IP injection of 0.2 mL 50% glucose. Human C-peptide ELISA was performed as directed (Mercodia, Sweden) and if necessary, samples were diluted to fall within the range of the calibration curve.

Histology and Immunohistochemistry

Explanted devices, engrafted subcutaneous tissue, engrafted kidneys, and pancreases were harvested from killed mice, fixed in 4% paraformaldehyde (USB, OH), and embedded in optimal cutting temperature (OCT) freezing media (Sakura Finetek, CA) or in paraffin. Sample sections were 5 μm. Paraffin sections were treated by alcohol series and antigen retrieval with CitriSolv (Fisher Scientific, PA). Primary antibodies used were directed against luciferase, CD3, insulin and somatostatin (Santa Cruz biotechnology, CA), Ki67 (Abcam, MA and DAKO, Denmark), CK19 (DAKO), and glucagon (BD, CA and Sigma). Apoptosis was studied with ApopTag Red In Situ Apoptosis Kit (Chemicon, CA). For fluorescent imaging, samples were incubated with Alexa 488 (Invitrogen, CA) or rhodamine (Jackson Immuno Research, PA) fluor-labeled anti-goat, -mouse, -rabbit, or -rat and nuclear counterstained with 4′, 6-diamidino-2-phenylindole (DAPI) (Invitrogen). Controls using irrelevant primary antibodies or secondary antibodies alone were used to ensure specificity of immunostaining. Brightfield and fluorescently labeled sections were analyzed with a conventional inverted microscope (Olympus, PlanFl 40×/0.60, Center Valley, PA) or with a confocal microscope (Bio-Rad Laboratories Inc., CA) equipped with krypton/argon laser. Examination of immunohistochemistry was performed by at least two blinded observers. The sectioning of the device damaged some tissue sections and these were discarded. Thus, for technical reasons, absolute cell counts per device were not determined. Quantitation of pixel intensity was performed with Image J software.

Bioluminescent Imaging

For in vitro studies, encapsulated luciferase expressing melanoma cells were placed in tissue culture media and imaged before and after addition of firefly-D-luciferin. Imaging was conducted using a cryogenically cooled IVIS 100 imaging system and data acquisition computer with Living Image Software (Xenogen) (see Figure, Supplemental Digital Content 1, http://links.lww.com/A931).

For in vivo studies, anesthetized mice were injected IP with 150 mg/kg firefly-D-luciferin, 10 min before imaging. In vivo bioluminescent images appear larger than the device size because of spreading of the signal from the source to the skin surface. The integrated BLI signal on the day of transplantation (day 0) was assigned a value of 100%.

Statistical Analyses

Data are presented as means±SEM. The statistical significance of the differences between groups was analyzed by Student's *t* tests except for Kaplan-Meier survival curves in NOD studies, which were analyzed by log-rank tests.

RESULTS

Human Fetal β-Cells/Precursors Thrive Within an Immunoisolation Device

To study the survival, function, and differentiation of encapsulated human β-cells and their progenitors, ICCs were prepared from 18- to 22-week-old human fetal pancreases. A portion of the cells were analyzed by immunohistochemistry and we determined that the fraction of insulin positive cells (ins+) in starting material was7% ± 1.2%, similar to previous reports (37). Encapsulated human ICCs were transplanted subcutaneously. As a control for tissue integrity, an equal number of nonencapsulated ICCs from each preparation were transplanted into the RC where they have been shown to acquire glucose responsiveness after a length of time that approximates term gestation (37,38). Immunodeficient SCID-Beige mice were used for these studies as they were directed at the survival and function of transplanted human cells, rather than the protection of human ICCs from xenograft rejection.

Grafted cells were harvested from five ICC preparations after 10 weeks of transplantation. Insulin, glucagon, and somatostatin expressing cells were readily identified in control and encapsulated grafts (Fig. 1A,B). In fact, during transplantation, the fraction of ins+ cells in devices nearly tripled, rising to 19%±2.7% (P<0.01) (Fig. 1C).

Evidence for β-Cell Replication and Neogenesis in Encapsulated Human Fetal Tissue

During human pancreatic development, both neogenesis and replication (39) play important roles in the regulation of endocrine cell formation. These processes are recapitulated in human ICCs transplanted into the RC of mice (40). Thus, we examined whether a combination of β-cell replication and neogenesis from precursors was also responsible for the striking increase in β-cell fraction we observed in encapsulated ICCs.

To determine the mitotic index of β-cells in the grafts, we performed immunohistochemical analysis for the proliferation marker Ki67 and insulin. Similar to previous reports, the mitotic index of ins+ cells in control, nonencapsulated RC transplants was 1.0%. Strikingly, the percent of replicating cells in the encapsulated ICCs grafts was 3.6% (P<0.05) (Fig. 1D,E), indicating that the microenvironment within the device is not only permissive for fetal β-cell replication, but may actually promote it.

During β-cell neogenesis, new β-cells budding from ducts transiently coexpress insulin and the duct cytokeratin, CK19, whereas in the adult pancreas, expression of insulin and CK19, are normally restricted to β-cells and duct cells, respectively (41). Insulin and CK19 double-positive cells can also be identified in grafts harvested from ICCs transplanted into the RC (Fig. 2A,B) (40). We investigated whether this intermediate cell type, suggestive of active β-cell differentiation, also existed in encapsulated ICCs, with the finding that CK19 and insulin coexpressing cells, as well as both single-positive cell types were readily identified (Fig. 2A,B). Taken together, these data suggest that both neogenesis and β-cell replication occur in encapsulated ICCs as they do in ICCs transplanted into the RC.

Encapsulated Human Fetal β-Cells Mature and Ameliorate Diabetes in Alloxan-Treated Mice

The hallmark of β-cell maturation is acquisition of glucose responsive insulin secretion, which can be monitored by measuring circulating human C-peptide levels as a surrogate for insulin. Five of seven encapsulated ICC preparations led to measurable C-peptide. In the first 12 weeks

after transplantation of encapsulated human ICCs, plasma C-peptide levels were low and did not change in response to a glucose challenge. However, when tested again at 5 months after transplantation, the same mice exhibited increased basal C-peptide levels and glucose responsiveness (Fig. 2C), indicating that β-cell maturation had occurred inside the device (P<0.01). RC control transplants also displayed glucose responsive insulin secretion, with C-peptide values approximately threefold higher than encapsulated cells (data not shown).

We estimated that devices contained a maximum of 70 IEQ at maturation. Although this number is far below the 300 islets required to cure diabetes in mice, we hypothesized that the transplanted cells would contribute to glucose homeostasis. Therefore, we eliminated murine β-cells by administration of alloxan, a drug selectively toxic to murine, but not human β-cells (34). Within 48 hr after alloxan treatment, untransplanted mice became diabetic while, in mice transplanted with encapsulated ICCs 5 months earlier, diabetes was attenuated for at least 10 days after alloxan treatment (Fig. 2D) (P<0.05).

Subsequent device removal resulted in a marked increase in blood glucose, demonstrating that encapsulated human cells, not residual murine cells, were responsible for glycemic control (see Figure, Supplemental Digital Content 2, http://links.lww.com/A933). Further, analysis of explanted pancreases ensured that alloxan-mediated murine β-cell destruction had taken place (data not shown).

Encapsulated Human Adult Islets Exhibit Poor Survival, but Remaining Cells Are Glucose Responsive

We next evaluated the survival of encapsulated human adult islets. Although equal numbers (approximately 216 IEQ, see Methods section) of islets were transplanted in devices or RC controls, C -peptide levels from device transplanted animals were merely 5% that of controls (P<0.01) at 1 month posttransplant (Fig. 3A). Remaining encapsulated islets retained glucose responsiveness but were not sufficient to alleviate alloxan-induced diabetes. In contrast, recipients of control RC transplants remained normoglycemic after alloxan treatment (Fig. 3B). Unlike human ICCs, which exhibited substantial increases in C-peptide production over time, no increase was observed from adult human islets measured again at 3 months (data not shown). In fact, tissue could not be found in most harvested devices, suggesting that cell death was the major barrier to successful transplantation outcome.

Real-Time Assessment of Graft Survival and Engraftment Kinetics

The finding that encapsulated human fetal ICCs survived well suggested that fetal tissue was resistant to cell death, or that it also underwent cell loss immediately posttransplant but was capable of repopulating the device. We could not distinguish between the two models by measuring C-peptide from ICCs as C-peptide was below the level of detection at the time of transplantation. Because we could not follow human ICC engraftment at early stages, we used BLI of encapsulated neonatal murine islets for real-time analysis of the engraftment process (30,42).

Encapsulated FVB strain islets expressing luciferase (FVB^{luc}) were transplanted into 12 wtFVB mice and imaged over the course of 50 days (Fig. 4A,B). Imaging on day 7 revealed a 68.7% loss in overall tissue survival compared with the day of transplantation. The declining trend reversed, however, such that by day 47, the BLI signal was restored to initial values (day 0 compared with day 47, $P = 0.9$). The data provided evidence that engraftment of young tissue is a dynamic process involving cell death and regrowth (Fig. 4C). Immunohistochemical analysis of insulin expression in devices harvested at day 50 revealed that β-cells represented 28.4%±8.4% of the total cell population (Fig. 5C).

Real-Time Analysis of Allograft Survival in Encapsulated Murine Neonatal Islets

To monitor cell survival of allografts in real time, neonatal islets from FVB^{luc} mice were transplanted across the major histocompatibility complex barrier into ICR strain mice (Fig. 4D). Similar to transplants into wtFVB mice, BLI revealed a 50% drop in signal at day 7, which was restored to the original value by day 21 (Fig. 4E) demonstrating complete protection of transplanted tissue. Immunohistochemical analysis of devices harvested at day 50 revealed that insulin was expressed in 21%±5.4% of the cells (Fig. 5C). Encapsulated islets retained BLI signal in ICR mice for as long as they were monitored (> 140 days) (Fig. 4E). As expected, the BLI signal disappeared from unprotected control transplants within 21 days, (Fig. 4D), and histologic examination confirmed that the no graft remained after signal disappeared (data not shown).

Encapsulated β-cells Are Protected From Autoimmune Rejection in a Model of Type I Diabetes

We next addressed whether primary murine islets could be protected from both auto- and alloimmune rejection in the NOD mouse model of type I diabetes (43). We found that encapsulated murine FVB^{luc} islets retained BLI, indicating overall graft survival, for greater than 50 days (Fig. 5A). Immunohistochemical examination of explanted devices revealed abundant insulin and glucagon expression (Fig. 5B), with β-cells representing 26.3%±8.0% of the total cell population (Fig. 5C), and a mitotic index, which was similar to cells in devices harvested from FVB and ICR host animals (Fig. 5D). No apoptotic cells were observed in devices harvested from FVB, ICR, or NOD mice (data not shown). In contrast, BLI revealed that unprotected islets were rejected within 28 days, as expected (Fig. 5A).

We hypothesized that the encapsulated β-cells (approximately 94 IEQ, see Methods) would be capable of partially, but not fully, ameliorating hyperglycemia in NOD mice. Thus, the rate of diabetes induction in NOD mice transplanted with encapsulated islets was compared with control untransplanted NOD mice. A single treatment of low-dose streptozotocin was administered at day 0 to accelerate autoimmune disease (35,36). Unlike high-dose alloxan, which causes massive β-cell death and hyperglycemia within 24 to 48 hr (Fig. 2D), this low-dose treatment did not affect glycemia in the first week. Importantly, NOD mice transplanted with encapsulated islets (n = 8) developed diabetes at a significantly lower rate than control untransplanted mice (n = 7, $P = 0.021$) (Fig. 5I). Thus, encapsulated β-cells were protected from both allo- and autoimmune rejection and functioned to slow the progression of diabetes in NOD mice.

T-Cell Recruitment Is not Elicited by Encapsulated Primary β-Cells

Recently, we reported improved survival of endogenous β-cells in the NOD pancreas when T cells were confined to the islet periphery by administration of a matrix metalloproteinase inhibitor (44). To determine whether encapsulated primary β-cells were protected from immune destruction by simple barrier exclusion of immune effector cells or whether encapsulation curtailed graft recognition by the immune system, we performed immunohistochemical analysis for CD3 positive cells in the tissue peripheral to devices. Of great significance, we determined that T cells were absent within 600 μm of devices (the greatest distance analyzed) (Fig. 5E), whereas pancreas tissue concurrently analyzed from the same NOD mice exhibited fulminate autoimmune disease: masses of lymphocytes, including CD3 positive T cells, and a 90% or greater loss of endogenous β-cells (Fig. 5F–H). Thus, encapsulated β-cells seemed to have evaded T-cell recognition.

DISCUSSION

Our studies demonstrate for the first time that human β-cells survive, differentiate, and function within a durable immunoisolation device. We observed a temporal increase in β-cell fraction with evidence of replication in encapsulated human ICCs. Further, the development of glucose responsive insulin secretion represents β-cell maturation from either immature β-cells or earlier pancreatic endocrine progenitors in the device.

Novocell has recently described a method for the production of hES-derived pancreatic precursors (45) that efficiently generate functional β-cells in vivo (46). Our data demonstrating that human fetal pancreatic progenitors are capable of maturing inside the device suggest that maturation of encapsulated hES-derived pancreatic progenitors may also occur. Importantly, a durable immunoisolation device could provide a platform for safely evaluating such cell-based therapies clinically, by protecting patients from any risk of potential tumorigenicity from the transplanted cells.

Encapsulated adult human islets exhibited relatively poor survival. This was not surprising given that adult human islet survival is suboptimal even in clinical islet transplantation (23–25). Importantly, however, surviving encapsulated adult islets retained glucose-stimulated insulin release. Thus, once established, adult human β-cells function normally in the device. The use of antiapoptotic drugs to prevent cell death in clinical islet transplantation seems promising and may be beneficial to encapsulated human islet cells as well (47).

We explored the underlying mechanism responsible for the robust survival and performance of encapsulated β-cell precursors using BLI. We expected that young tissue might be resistant to cell death immediately posttransplant and therefore would exhibit a constant BLI signal. We determined, however, that young islets undergo significant cell death immediately posttransplant, followed by recovery of cell mass, suggesting an important role for replication in their performance. Other factors which may influence ICC versus adult islet survival are tissue ischemic time, or differences in the growth factors, cytokines, or blood vessels induced by young versus older tissue.

In past studies assessing the immunoprotective features of the device, survival of encapsulated cells was qualitatively assessed or inferred by counting cells in a number of sections of harvested grafts. For a precise quantitative evaluation of graft survival, we again employed BLI. We limited our studies to allograft and autoimmune protection because reports that the device provided xenograft protection (17–19) were not confirmed by others (10–22, and personal communication). The device provided protection from allograft rejection for greater than 140 days, a finding immediately applicable to transplantation therapies for type II or monogenetic maturity onset diabetes of the young (MODY) diabetes. We also undertook a careful and quantitative analysis of encapsulated allografts in the NOD model of autoimmune (type I) diabetes, finding that the device provided significant protection, allowing amelioration of hyperglycemia. Complete reversal of diabetes was not expected in these studies because of the limited number of β-cells in the transplanted devices. It is possible that graft survival could have been extended by controlling hyperglycemia with exogenous insulin treatment. Importantly, in islet transplant patients who require some exogenous insulin for glycemic control, even subcurative numbers of β-cells provide substantial clinical benefit (23,48).

In transplanted NOD mice, T cells were not recruited to the tissue surrounding the device. This was somewhat surprising, given that severe insulitis was readily apparent in pancreases from the same mice. The data suggest that the encapsulated β-cells are invisible to the immune system and this bodes well for long-term clinical translation of the technology. In contrast to our work, in a study in which an insulinoma cell line was similarly encapsulated and transplanted into NOD mice, T cells were observed proximal to the devices (31). This disparity

may result from the high-cell turnover of a transformed line generating increased antigen shedding, and therefore, immune stimulation.

Taken together, our data suggest that long-term protection of human β-cells in type I diabetic patients without immunosuppression is a realistic goal. Further, encapsulation of β-cell precursors may be an ideal approach to enhance the success of β-cell replacement therapies.

ACKNOWLEDGMENTS

The authors thank Ling Wang, Taylor Williams, Buddy Charbono, Mary Braxton, and Lloyd Slivka for excellent technical assistance, Bruce Worcester for critical reading of the manuscript, and Ed Monosov, Tom Loudovaris, and Jim Brauker for helpful discussion.

This work was supported by grants from JDRF and the J. W. Kieckhefer Foundation.

REFERENCES

1. Nir T, Melton DA, Dor Y. Recovery from diabetes in mice by beta cell regeneration. J Clin Invest 2007;117:2553. [PubMed: 17786244]
2. Murakami M, Satou H, Kimura T, et al. Effects of micro-encapsulation on morphology and endocrine function of cryopreserved neonatal porcine islet-like cell clusters. Transplantation 2000;70:1143. [PubMed: 11063331]
3. Barnett BP, Arepally A, Karmarkar PV, et al. Magnetic resonance-guided, real-time targeted delivery and imaging of magnetocapsules immunoprotecting pancreatic islet cells. Nat Med 2007;13:986. [PubMed: 17660829]
4. Schneider S, Feilen PJ, Brunnenmeier F, et al. Long-term graft function of adult rat and human islets encapsulated in novel alginate-based microcapsules after transplantation in immunocompetent diabetic mice. Diabetes 2005;54:687. [PubMed: 15734844]
5. Beck J, Angus R, Madsen B, et al. Islet encapsulation: Strategies to enhance islet cell functions. Tissue Eng 2007;13:589. [PubMed: 17518605]
6. Czyz J, Wiese C, Rolletschek A, et al. Potential of embryonic and adult stem cells in vitro. Biol Chem 2003;384:1391. [PubMed: 14669982]
7. Maitra A, Arking DE, Shivapurkar N, et al. Genomic alterations in cultured human embryonic stem cells. Nat Genet 2005;37:1099. [PubMed: 16142235]
8. Dufrane D, Goebbels RM, Saliez A, et al. Six-month survival of microencapsulated pig islets and alginate biocompatibility in primates: Proof of concept. Transplantation 2006;81:1345. [PubMed: 16699465]
9. Lee DY, Park SJ, Nam JH, et al. A new strategy toward improving immunoprotection in cell therapy for diabetes mellitus: Long-functioning PEGylated islets in vivo. Tissue Eng 2006;12:615. [PubMed: 16579694]
10. Thu B, Bruheim P, Espevik T, et al. Alginate polycation microcapsules. II. Some functional properties. Biomaterials 1996;17:1069. [PubMed: 8718966]
11. Brauker JH, Carr-Brendel VE, Martinson LA, et al. Neovascularization of synthetic membranes directed by membrane microarchitecture. J Biomed Mater Res 1995;29:1517. [PubMed: 8600142]
12. Geller RL, Neuenfeldt S, Levon SA, et al. Immunoisolation of tumor cells: Generation of antitumor immunity through indirect presentation of antigen. J Immunother 1997;20:131. [PubMed: 9087385]
13. Geller RL, Loudovaris T, Neuenfeldt S, et al. Use of an immunoisolation device for cell transplantation and tumor immunotherapy. Ann N Y Acad Sci 1997;831:438. [PubMed: 9616733]
14. Tibell A, Rafael E, Wennberg L, et al. Survival of macroencapsulated allogeneic parathyroid tissue one year after transplantation in nonimmunosuppressed humans. Cell Transplant 2001;10:591. [PubMed: 11714193]
15. Rafael E, Wu GS, Hultenby K, et al. Improved survival of macroencapsulated islets of Langerhans by preimplantation of the immunoisolating device: A morphometric study. Cell Transplant 2003;12:407. [PubMed: 12911128]

16. Suzuki K, Bonner-Weir S, Hollister-Lock J, et al. Number and volume of islets transplanted in immunobarrier devices. Cell Transplant 1998;7:47. [PubMed: 9489762]
17. Yang Z, Chen M, Fialkow LB, et al. Survival of pancreatic islet xenografts in NOD mice with the theracyte device. Transplant Proc 2002;34:3349. [PubMed: 12493470]
18. Chou FF, Huang SC, Chen SS, et al. Treatment of osteoporosis with TheraCyte-encapsulated parathyroid cells: A study in a rat model. Osteoporos Int 2006;17:936. [PubMed: 16596462]
19. Garkavenko O, Emerich DF, Muzina M, et al. Xenotransplantation of neonatal porcine liver cells. Transplant Proc 2005;37:477. [PubMed: 15808681]
20. Brauker J, Martinson LA, Young SK, et al. Local inflammatory response around diffusion chambers containing xenografts. Nonspecific destruction of tissues and decreased local vascularization. Transplantation 1996;61:1671. [PubMed: 8685942]
21. Colton CK. Implantable biohybrid artificial organs. Cell Transplant 1995;4:415. [PubMed: 7582573]
22. McKenzie AW, Georgiou HM, Zhan Y, et al. Protection of xenografts by a combination of immunoisolation and a single dose of anti-CD4 antibody. Cell Transplant 2001;10:183. [PubMed: 11332633]
23. Ryan EA, Paty BW, Senior PA, et al. Five-year follow-up after clinical islet transplantation. Diabetes 2005;54:2060. [PubMed: 15983207]
24. Emamaullee JA, Shapiro AM. Factors influencing the loss of beta-cell mass in islet transplantation. Cell Transplant 2007;16:1. [PubMed: 17436849]
25. Keymeulen B, Gillard P, Mathieu C, et al. Correlation between beta cell mass and glycemic control in type 1 diabetic recipients of islet cell graft. Proc Natl Acad Sci USA 2006;103:17444. [PubMed: 17090674]
26. Itkin-Ansari P, Geron I, Hao E, et al. Cell-based therapies for diabetes: progress towards a transplantable human beta cell line. Ann N Y Acad Sci 2003;1005:138. [PubMed: 14679048]
27. Hayek A, Beattie GM. Experimental transplantation of human fetal and adult pancreatic islets. J Clin Endocrinol Metab 1997;82:2471. [PubMed: 9253320]
28. Beattie GM, Otonkoski T, Lopez AD, et al. Functional beta-cell mass after transplantation of human fetal pancreatic cells: Differentiation or proliferation? Diabetes 1997;46:244. [PubMed: 9000701]
29. Wang S, Beattie GM, Mally MI, et al. Isolation and characterization of a cell line from the epithelial cells of the human fetal pancreas. Cell Transplant 1997;6:59. [PubMed: 9040956]
30. Cao YA, Bachmann MH, Beilhack A, et al. Molecular imaging using labeled donor tissues reveals patterns of engraftment, rejection, and survival in transplantation. Transplantation 2005;80:134. [PubMed: 16003245]
31. Loudovaris T, Jacobs S, Young S, et al. Correction of diabetic nod mice with insulinomas implanted within Baxter immunoisolation devices. J Mol Med 1999;77:219. [PubMed: 9930967]
32. Tatarkiewicz K, Hollister-Lock J, Quickel RR, et al. Subcutaneous transplantation of rat islets into diabetic nude. Transplant Proc 1998;30:479. [PubMed: 9532136]
33. Elliott RB, Escobar L, Calafiore R, et al. Transplantation of micro- and macroencapsulated piglet islets into mice and monkeys. Transplant Proc 2005;37:466. [PubMed: 15808678]
34. Tyrberg B, Andersson A, Borg LA. Species differences in susceptibility of transplanted and cultured pancreatic islets to the β-cell toxin alloxan. Gen Comp Endocrinol 2001;122:238. [PubMed: 11356036]
35. Horwitz MS, Ilic A, Fine C, et al. Presented antigen from damaged pancreatic beta cells activates autoreactive T cells in virus-mediated autoimmune diabetes. J Clin Invest 2002;109:79. [PubMed: 11781353]
36. Krishnamurthy B, Mariana L, Gellert SA, et al. Autoimmunity to both proinsulin and igrp is required for diabetes in nonobese diabetic 8.3 TCR transgenic mice. J Immunol 2008;180:4458. [PubMed: 18354167]
37. Beattie GM, Levine F, Mally MI, et al. Acid beta-galactosidase: A developmentally regulated marker of endocrine cell precursors in the human fetal pancreas. J Clin Endocrinol Metab 1994;78:1232. [PubMed: 8175983]
38. Kemp CB, Knight MJ, Scharp DW, et al. Effect of transplantation site on the results of pancreatic islet isografts in diabetic rats. Diabetologia 1973;9:486. [PubMed: 4204180]

39. Bouwens L, Lu WG, De Krijger R. Proliferation and differentiation in the human fetal endocrine pancreas. Diabetologia 1997;40:398. [PubMed: 9112016]
40. Tuch BE, Ng AB, Jones A, et al. Histologic differentiation of human fetal pancreatic explants transplanted into nude mice. Diabetes 1984;33:1180. [PubMed: 6149970]
41. Bonner-Weir S, Baxter LA, Schuppin GT, et al. A second pathway for regeneration of adult exocrine and endocrine pancreas. A possible recapitulation of embryonic development. Diabetes 1993;42:1715. [PubMed: 8243817]
42. Lu Y, Dang H, Middleton B, et al. Bioluminescent monitoring of islet graft survival after transplantation. Mol Ther 2004;9:428. [PubMed: 15006610]
43. Kikutani H, Makino S. The murine autoimmune diabetes model:NOD and related strains. Adv Immunol 1992;51:285. [PubMed: 1323922]
44. Savinov AY, Rozanov DV, Golubkov VS, et al. Inhibition ofmembranetype-1 matrix metalloproteinase by cancer drugs interferes with the homing of diabetogenic T cells into the pancreas. J Biol Chem 2005;280:27755. [PubMed: 15944163]
45. D'Amour KA, Bang AG, Eliazer S, et al. Production of pancreatic hormone-expressing endocrine cells from human embryonic stem cells. Nat Biotechnol 2006;24:1392. [PubMed: 17053790]
46. Kroon E, Martinson LA, Kadoya K, et al. Pancreatic endoderm derived from human embryonic stem cells generates glucose-responsive insulin-secreting cells in vivo. Nat Biotechnol 2008;26:443. [PubMed: 18288110]
47. Emamaullee JA, Stanton L, Schur C, et al. Caspase inhibitor therapy enhances marginal mass islet graft survival and preserves long-term function in islet transplantation. Diabetes 2007;56:1289. [PubMed: 17303806]
48. Suzuki K, Bonner-Weir S, Trivedi N, et al. Function and survival of macroencapsulated syngeneic islets transplanted into streptozocin-diabetic mice. Transplantation 1998;66:21. [PubMed: 9679817]

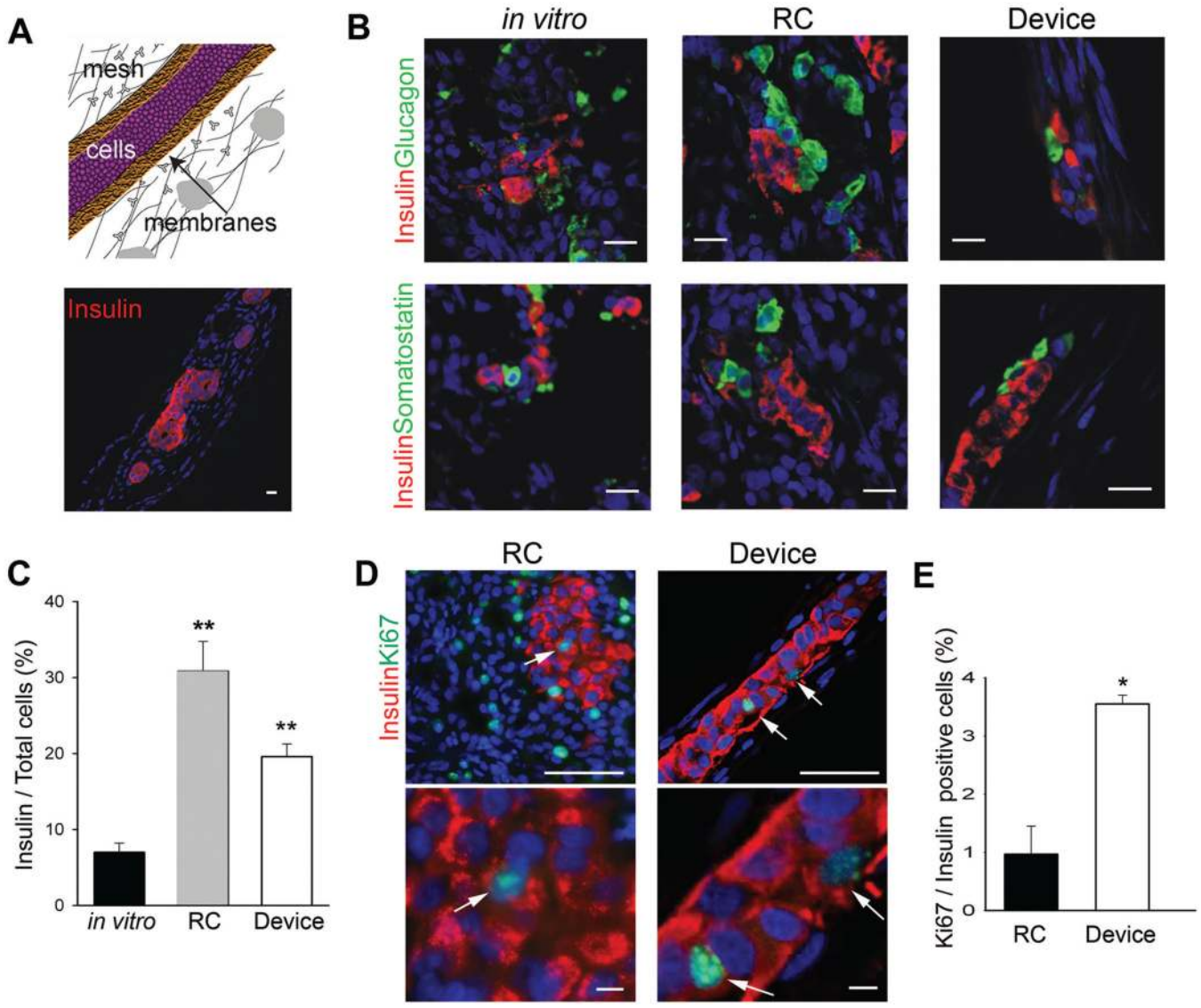

FIGURE 1.

Macroencapsulated β-cells derived from human fetal islet-like cell clusters (ICCs) survive and replicate. (A) Schematic representation of a cross section through a cell-filled TheraCyte encapsulation device; immunohistochemical analysis of a representative human ICC-filled device explanted 10 weeks after placement; insulin (*red*) n = 5, scale bar: 15 μm. (B) Immunohistochemical analysis of islet hormones; insulin (red), glucagon (*green*), and somatostatin (*green*) in human ICCs in vitro (n = 3), 10 weeks after transplantation into the renal compartment (RC, n = 3), or in device placed subcutaneously (Device, n = 5), scale bar: 15 μm. (C) Quantitation of insulin-positive cell fractions in human ICCs before (in vitro, n = 3, *black bar*) and 10 weeks after transplantation in device (Device, n = 3, *white bar*) or control transplantation (RC, n = 3, *gray bar*). (D) Immunostaining for insulin (*red*) and proliferation marker Ki67 (*green*) in devices or RC grafts explanted after 10 weeks. *Arrows* depict Ki67+/ insulin = cells, scale bar: 50 μm, magnified insets, scale bar: 5 μm. (E) Quantitation of mitotic index in control (RC, n = 3) and device transplants (Device, n = 3), *P* values *less than 0.05, **less than 0.01. Blue nuclear counterstain in A, B, and D is DAPI.

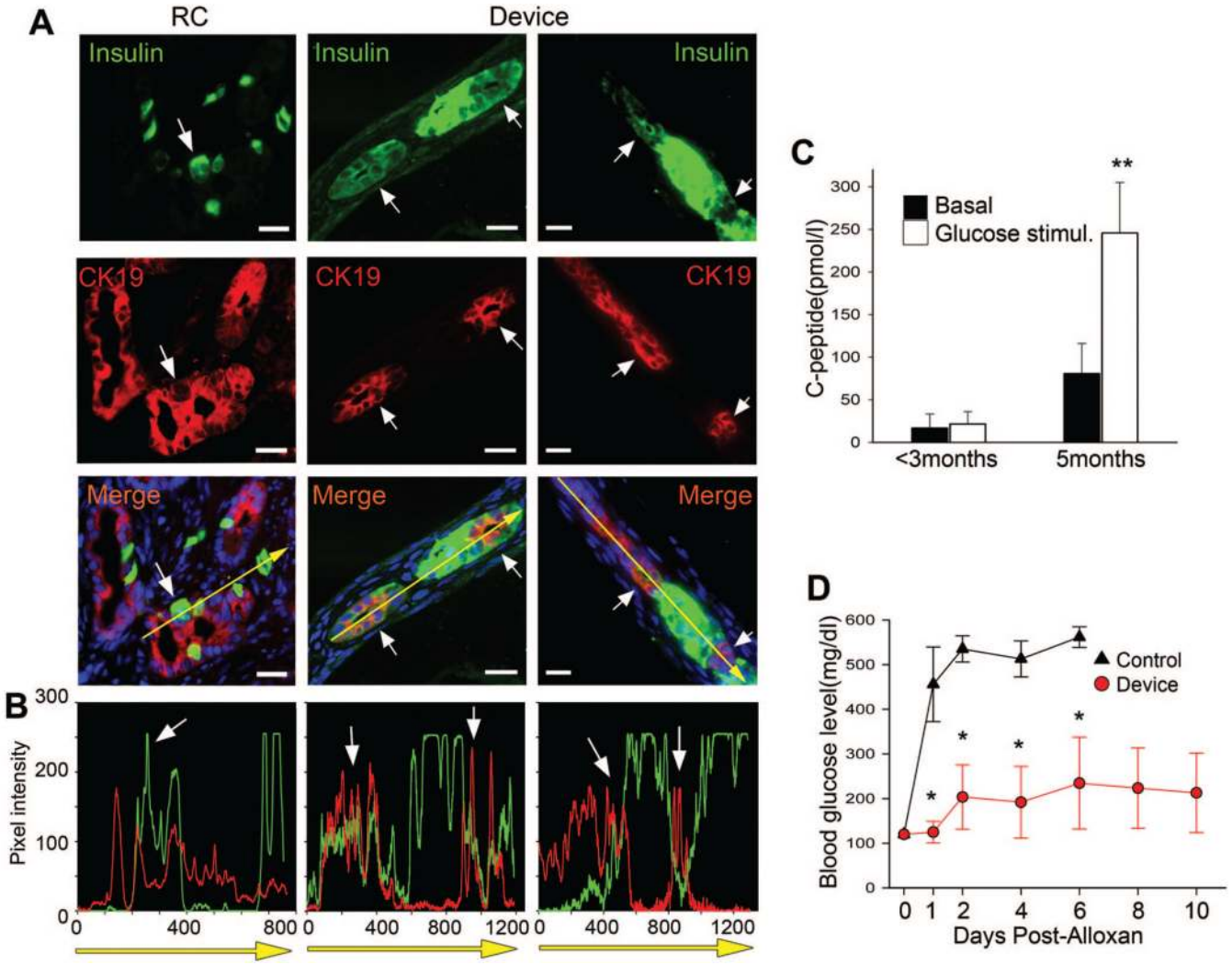

FIGURE 2.

Macroencapsulated β-cells derived from human fetal islet-like cell clusters (ICCs) mature and ameliorate diabetes. (A) Confocal images of immunostaining for insulin (*green*) and CK19 (*red*) in two encapsulated grafts (Device) and one renal compartment control graft of human ICCs harvested at 10 weeks posttransplant, reveals cells coexpressing insulin and CK19 (*arrows*), scale bar: 20 μm. (B) Graphs quantifying pixel intensity of insulin (*green*) and CK19 (*red*) expression (*white arrows* depict areas of coexpression) corresponding to direction of *yellow arrow* in merge pictures from A. (C) Human ICCs mature within an encapsulation device as exhibited by plasma human C-peptide levels measured at less than 3 months and again at 5 months in the same animals (n = 3). Basal level = *black bars* and *white bars* = level at 30 min after glucose stimulation. (D) Blood glucose levels were measured after alloxan administration in animals transplanted 5 months earlier with encapsulated ICCs (Device, *red circle*,n = 3) or in untransplanted mice (Control, *black triangles*, n = 9), *P* values *less than 0.05, **less than 0.01. Day-0 blood glucose (115 mg/dL±4.7 mg/dL) was average from 15 controls. Blue nuclear counterstain in A is DAPI.

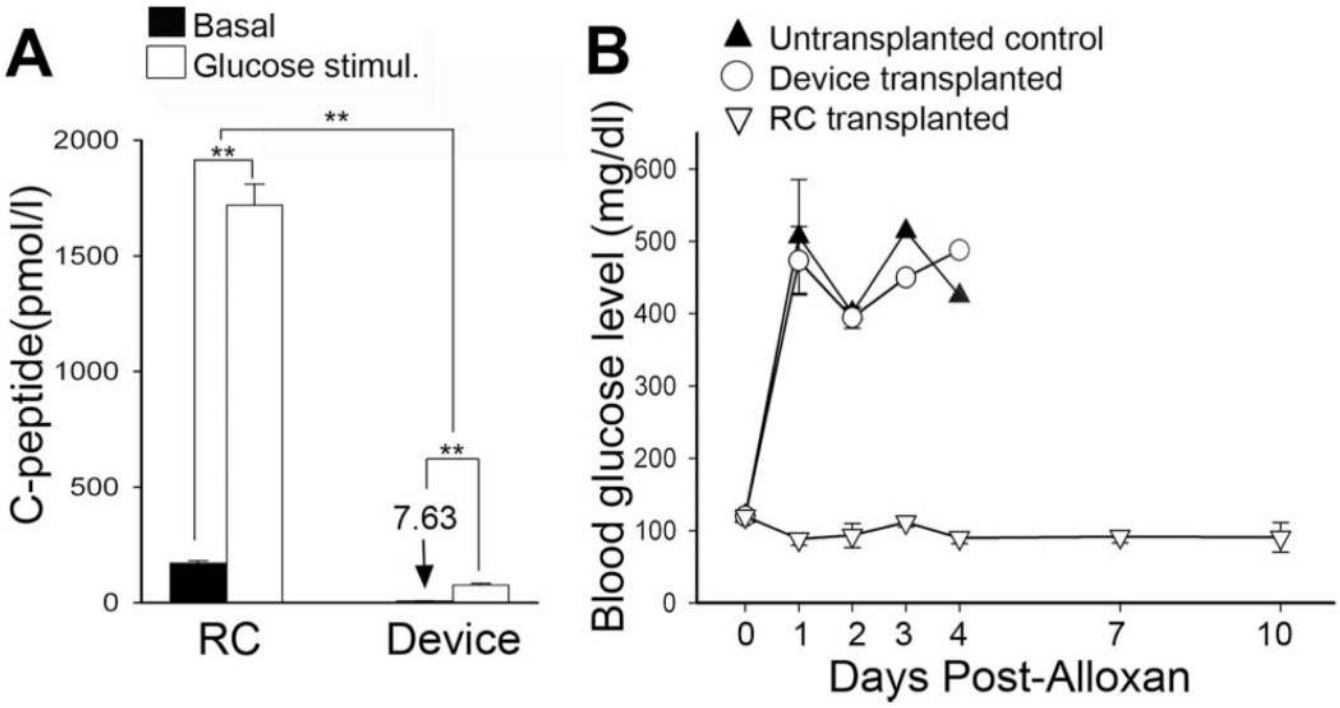

FIGURE 3.

Encapsulated human adult islets exhibit poor survival, but remaining cells are glucose responsive. (A) Plasma C-peptide level, was measured in mice transplanted 1 month earlier with human adult islets, either encapsulated (Device, n = 5) or nonencapsulated (renal compartment [RC], n = 5). Basal fasting C-peptide level was obtained after overnight fast (*black*), stimulated value was obtained 30 min after glucose bolus (*white*). (B) Blood glucose was measured after alloxan treatment (to ablate endogenous murine β-cells) in untransplanted control mice (*black triangle*), mice transplanted 1 month earlier with islets in RC (*open inverted triangle*), or mice transplanted with encapsulated islets (*open circle*) and n = 3 for each group, *P* values **less than 0.01. Day-0 blood glucose (115 mg/dL±4.7 mg/dL) is a mean of 15 control mice.

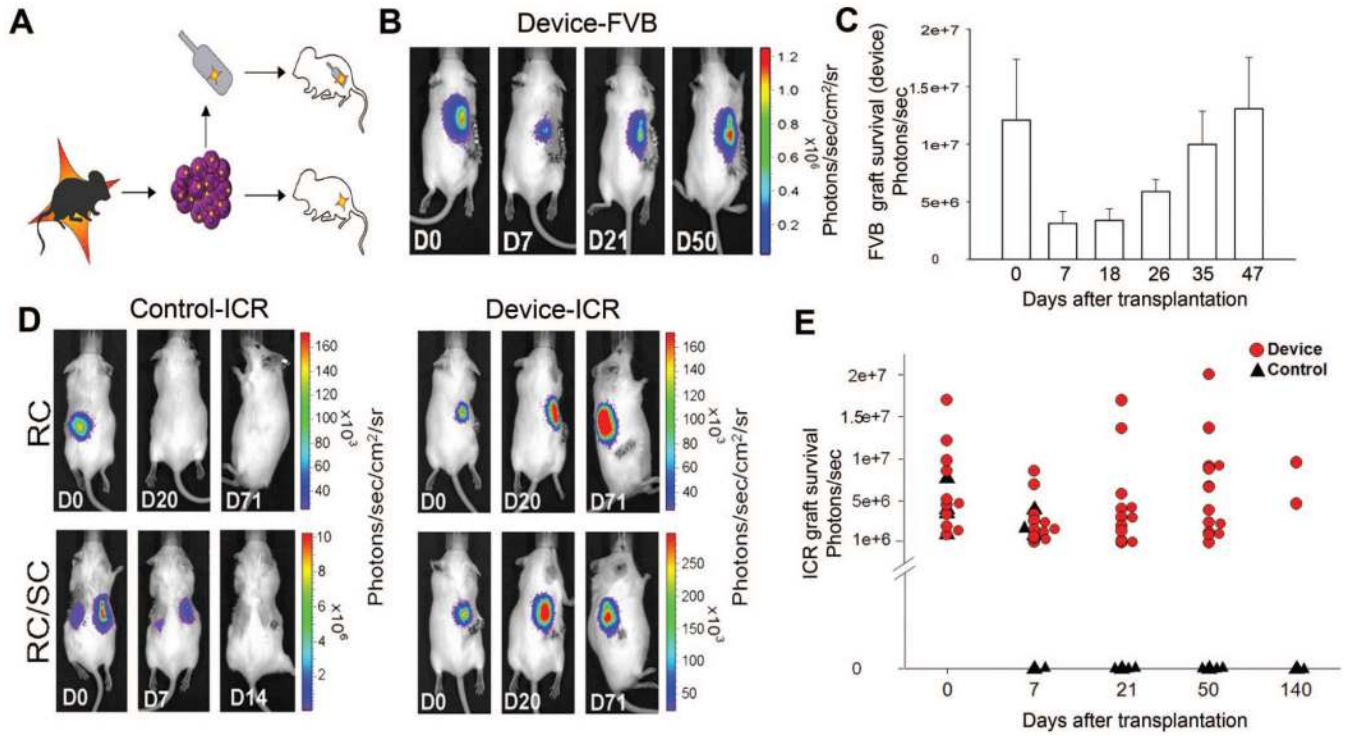

FIGURE 4.

Bioluminescent imaging (BLI) reveals kinetics of engraftment and allograft protection of encapsulated murine islets in real time. (A) Schematic diagram of experimental design for transplants of luciferase-expressing islets and (B) pseudocolor BLI of representative wtFVB mouse transplanted with encapsulated neonatal FVB^{luc} islets (Device, n = 12), imaged immediately after transplant (D0), and on subsequent days. (C) Quantitation of BLI signal. There is no significant difference in signal between day 0 and day 47 $P = 0.9$. (D) Representative BLI from islet allografts: FVB^{luc} islets transplanted into islet cell resources mice and control mice were transplanted with unencapsulated cells into renal compartment (RC) (n = 4). Two of the controls also have implants in contra-lateral subcutaneous tissue (RC/SC). Encapsulated islets were transplanted subcutaneously (Devices, n = 11). E: Quantitation of BLI signal: encapsulated cells (Device, *red circles*, n = 11) and control transplants (Control, *black triangles*, n = 4). All animals were monitored for 50 days; two device-transplanted animals and two controls were maintained for more than 140 days.

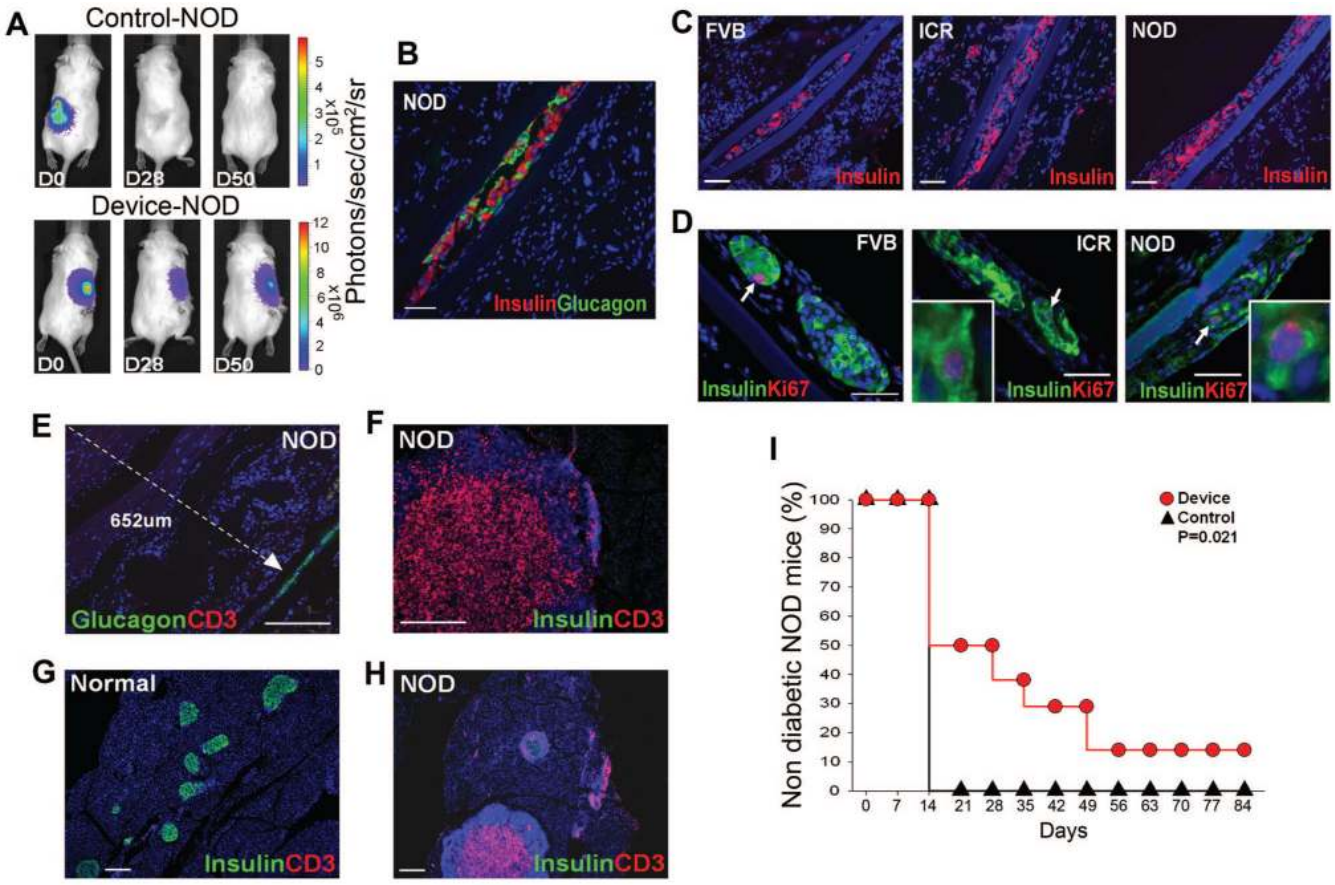

FIGURE 5.

Encapsulated islets survive and alleviate diabetes in NOD mice. (A) BLI of representative NOD mice transplanted with FVB^{luc} islets, unencapsulated (Control, n = 7) or encapsulated (Device, n = 8). Animals were imaged immediately after transplantation (D0) and subsequently. (B) Insulin (*red*) and glucagon (*green*) immunostaining of representative device retrieved from NOD mouse after 50 days of transplantation when blood glucose levels were above 300 mg/dL, scale bar: 50 μm. (C) FVB^{luc} islet-filled devices retrieved from wtFVB, islet cell resources, and NOD recipient mice and immunostained for insulin (*red*) reveal similar extent of β-cell survival in all strains, scale bar: 50 μm and (D) contain similar numbers of replicating β-cells (*white arrows*) as illustrated by immunostaining for insulin (green) and Ki67 (*red*), scale bar: 50 μm. Inset is higher magnification. (E) Immunostaining for glucagon (*green*) and T-cell marker CD3 (*red*) in device and surrounding tissue explanted from NOD mouse. Note that no T cells can be identified by anti-CD3 antibody (*red*) within 652 μm (*white dotted line*) of device (*white arrowhead*) (n = 10), scale bar: 200 μm. (F, H) Immunostaining for insulin (*green*) and T-cell marker CD3 (*red*) in pancreas from the same NOD mouse at (F) high and (H) low power, revealing massive CD3-positive infiltrates in pancreas, scale bar: 200 μm. (G) Normal pancreas, scale bar: 200 μm. (I) NOD mice transplanted with encapsulated islets (Device, *red circle*, n = 8) and untransplanted NOD mice (Control, *black triangle*, n = 7) received a single treatment of low-dose streptozotocin at day 0 to accelerate autoimmune diabetes (35,36), $P = 0.021$. Mice with encapsulated islets exhibited delayed onset of diabetes compared with control animals. Nondiabetic blood glucose level is less than 300 mg/dL. Blue nuclear counterstaining B to H is DAPI.